Sensing and Bio-Sensing Research 8 (2016) 31–35

Contents lists available at ScienceDirect

Sensing and Bio-Sensing Research

journal homepage: www.elsevier.com/locate/sbsr

A liquid crystal biosensor for specific detection of antigens

Piotr Popov [a], Lawrence W. Honaker [b,1], Edgar E. Kooijman [c], Elizabeth K. Mann [a], Antal I. Jákli [b,d,*]

[a] Department of Physics, Kent State University, Kent, OH 44242, USA
[b] Liquid Crystal Institute, Kent State University, Kent, OH 44242, USA
[c] Department of Biological Sciences, Kent State University, Kent, OH 44242, USA
[d] Complex Fluid Group, Wigner Research Centre, H-1525 Budapest, Hungary

ARTICLE INFO

Article history:
Received 19 October 2015
Received in revised form 21 March 2016
Accepted 30 March 2016
Available online xxxx

Keywords:
Liquid crystal
Specific sensing
Optical biosensor

ABSTRACT

Following the principle of the enzyme-linked immunosorbent assay (ELISA) pathogen detection method, we demonstrate specific sensing of goat Immunoglobulin G (IgG) by a nematic liquid crystal material. Sensing occurs via the visually-striking realignment of a pre-fabricated liquid crystal film, suspended in grids and coated with biotinylated lipids followed by biotinylated anti-goat IgG. Realignment occurs when the targeted goat IgG is added to the cell, but not when rat or rabbit serum IgG is added to the same surface. In principle, this method can be generalized to provide an inexpensive, fast and sensitive prefabricated sensor for any pathogen.

1. Introduction

Currently, the most widespread technique to detect antigens is enzyme-linked immunosorbent assay (ELISA). This method uses a cascade of interactions between antibodies and antigens leading to a visual response that indicates the presence or absence of a given antigen or substance [1]. There are several different ELISA methods, such as direct and sandwich assays [2–4], but the underlying feature is the requirement for antibody–antigen binding to a surface followed by a secondary reaction to produce a response. This multi-step process always starts by binding the target antigen, either directly or via a capture antibody, to the surface of the assay chamber. The next step is blocking unbound sites with an unrelated protein-based solution. The third step is detection, where an antibody, conjugated with an enzyme such as horseradish peroxidase (HPR), binds the target antigen. The addition of a chromogenic substrate for the enzyme then creates a quantifiable signal. Washing processes separate each of these steps. Therefore, ELISA is a relatively lengthy process typically performed in a laboratory environment. Examples for other developing techniques for biosensors include surface plasmon resonance (SPR) [5] and microfluidics [6].

Liquid crystal materials have been used recently in a wide array of sensing applications that exploit the high sensitivity of their alignment to the conditions of surrounding immiscible media. Combined with the optical anisotropy of liquid crystals, this sensitivity produces a rapid, easily-visualized response. One of these techniques uses an aqueous non-toxic chromonic liquid crystal medium that reveals defects when an object in the medium is larger than the extrapolation length b, defined as the ratio of the director curvature elastic constant K and the anchoring strength W between the object and the liquid crystal medium [7,8]. If the size of the microbe before binding is smaller than b, but becomes larger after binding, a defect appears that can be detected optically. This technique, currently being developed by Crystal Diagnostics, Ltd. [9], provides rapid and selective identification of microbes.

The other type of liquid crystal-based sensing technique, pioneered by Abbott [10–14], utilizes realignment of the liquid crystal caused by absorption or desorption of surfactants at the LC-water interface. Pure water aligns the LC molecules to lie along the interface, whereas surfactants align them orthogonal to it. Although this technique has been demonstrated to be sensitive to a wide array of surfactants, lipids, DNA and proteins [15–19], it is very challenging to achieve the specific sensing of pathogens. In one variation of the techniques used by the Abbott group, solid surfaces are first functionalized with a layer that binds specifically to an antigen, and then any binding is detected by using the surface as an alignment layer for liquid crystal films. For example, the surface might be coated with biotinylated bovine serum albumin (BSA) that blocks non-specific adsorption of biological molecules but can bind to anti-biotin antigens, such as immunoglobulin G (IgG) [20]. A recent variant of specific detection used an antibody- or BSA-decorated LC aqueous interface. The LC alignment was shown to vary with specific interaction between vesicles and the antibody adsorbed at the LC interfaces [18].

None of these specific sensing methods offer a prefabricated sensor that can simply be brought into contact with an aqueous medium containing the antigen to be detected. A new pathogen detector in which

* Corresponding author at: Liquid Crystal Institute, Kent State University, Kent, OH 44242, USA.
E-mail address: ajakli@kent.edu (A.I. Jákli).
[1] Current affiliation: Physics and Materials Science Research Unit, University of Luxembourg, L-1511 Luxembourg, Grand Duchy of Luxembourg.

http://dx.doi.org/10.1016/j.sbsr.2016.03.008

the functionalized test substrates are made prior to the addition of the target antigen and the visualization can be done in remote locations, without the need of a laboratory environment, would be a significant advance. In this paper, we describe such a prefabricated sensor that holds the promise of providing inexpensive biosensors capable of visual confirmation of the presence of an antigen remote from any laboratory. We test this sensor design with several biomolecules, including controls.

2. Materials and methods

The liquid crystal used in our experiments, 4-cyano-4′-pentylbiphenyl (5CB, >99%), was obtained from Sigma Aldrich and used without further purification. However, any other nematic liquid crystal at convenient temperature ranges should be similarly useful. The lipids used were 1,2-dilauroyl-*sn*-glycero-3-phosphocholine (DLPC; Avanti Polar Lipids, >99%) and a triethylammonium salt of N-((6-(biotinoyl)amino)hexanoyl)-1,2-dihexadecanoyl-*sn*-glycero-3-phosphoethanolamine (Biotin-X-DHPE; Life Technologies); both were supplied in the form of powders and used without further purification.

The mixed Biotin-X-DHPE and DLPC vesicles were prepared according to Patil and Jadhav [21]. The lipid powders were dissolved in reagent-grade chloroform (>99%, Sigma Aldrich) to prepare lipid stocks of ~25 mg/ml. Lipid films were prepared by mixing appropriate amounts of the stock solution and allowing the chloroform to evaporate off under vacuum at 30 °C. After adding 5 ml of ultrapure deionized water, at a temperature slightly above the gel-liquid crystal transition temperature, the liposome dispersion typically appears cloudy, indicating the presence of MLVs. The dispersion was either tip-sonicated for 10 min using the pulsing mode or extruded through a 200 nm poly(tetrafluoroethylene) filter to leave a clear solution, indicated that vesicles are much smaller than visible light wavelengths. The observed changes in the liquid crystal films were the same with both treatments, both in pattern and in dynamics. Fig. 1 presents the molecular structures of the liquid crystal 5CB and the lipids.

Pierce™ NeutrAvidin (deglycosylated avidin) was obtained from Life Technologies and kept suspended in Tris buffer at a concentration of 2 mg/ml. Phosphate buffered saline (pH = 7.4) was prepared in ultrapure deionized water (resistivity of 18.2 MΩ·cm) obtained through a PureLab Plus™ system. The antibody attached to the interface was biotinylated anti-goat IgG produced from either mouse or donkey serum (Sigma Aldrich, salt-free lyophilized powder in bovine serum albumin), and this was used as a sensor for non-biotinylated IgGs obtained from goat, rat, and rabbit sera (Sigma Aldrich). All materials were used without further purification.

The experimental setup was recently described in detail [14]. Fig. 2(a) shows schematics of the setup. The liquid crystal sensor is placed between either crossed linear or left- and right-handed circular polarizers and imaged with a CCD camera mounted on an inverted microscope. The liquid crystal is smeared uniformly in one half of a Veco folding nickel 50/100 mesh 20-μm thick TEM grids with cell diameters

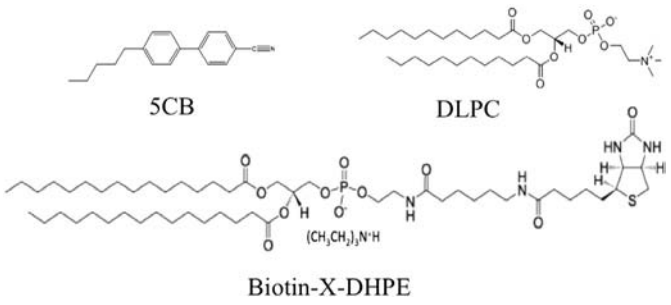

Fig. 1. Structures of 4-cyano-4′-pentylbiphenyl (5CB); 1,2-dilauroyl-sn-glycero-3-phosphocholine (DLPC); N-((6-(biotinoyl)amino)hexanoyl)-1,2-dihexadecanoyl-sn-glycero-3-phosphoethanolamine, triethylammonium salt (Biotin-X-DHPE).

in the range of 0.2–0.4 mm. The liquid crystal forms stable freestanding films in each grid cell. Tweezers hold this grid parallel to the bottom of the dish for the aqueous material. When both sides of the film are in contact with air, the average orientation of the liquid crystal molecules ("director") aligns perpendicular to the interfaces ("homeotropic" alignment), which appears dark between crossed linear or left- and right-handed circular polarizers. The dish is then filled with water to make contact with the bottom of the grid. Pure water promotes a director alignment parallel to the interface ("planar" alignment). Since the alignment is homeotropic on the air side, hybrid alignment results. Biologically relevant materials are then added to the water, which may change the alignment and the optical properties of the liquid crystal film, providing the basis of sensing. A close-up view of the liquid crystal between air and aqueous interfaces is shown schematically in Fig. 2(b). Since the aqueous solution is optically isotropic, the picture observed in the inverted polarizing microscope depends only on the alignment of the liquid crystal. With hybrid alignment, the texture appears uniformly bright and colored between circular polarizers and usually inhomogeneous between linear crossed polarizers because that configuration is sensitive to the lateral distribution of the optical axis [14].

Images were collected using a QI Fast1394 camera attached to a modified Olympus CK-40 polarizing optical microscope. This microscope is equipped with interchangeable linear and circular polarizers and a microstage to hold the sample in place and allow for minute adjustments of the position of the sample. The camera was, in turn, connected to a computer equipped with QI Capture software to collect and save images.

3. Results

When amphiphilic phospholipids, such as 1,2-dilauroyl-*sn*-glycero-3-phosphocholine (DLPC) are added to water, they migrate to the LC/water interface with tails embedded in the LC orthogonal to the interface while exposing their headgroups to the aqueous medium. At sufficiently high (>1 mM) concentrations of phospholipid in the medium, this process rapidly leads to homeotropic LC alignment both on the air and liquid side. Once the lipid is adsorbed to the surface, the TEM grid is removed from contact with the dispersion and placed on top of a drop of deionized water for five or more minutes to rinse away any unadsorbed lipid. DLPC monolayers covering the LC/water interface remain stable, as indicated by a dark texture showing homeotropic alignment at both the air and water interfaces, even after rinsing the film with pure water, indicating that the DLPC molecules bound to the liquid crystal interface do not desorb into pure water. However, when the DLPC-decorated LC surface is put in contact with the protein apoLp-III which binds to phospholipids [22], the texture brightens, thus indicating a change of the alignment from the aqueous side [23]. This reveals that a binding process of the apolipoprotein with DLPC can be visualized by liquid crystals and encouraged us to test the response of an antibody-decorated LC surface to its antigen.

To construct a decorated liquid crystal interface to respond to specific antigens, we employed biotin–avidin binding, an extremely strong interaction used in labeling of antibodies [24]. Fig. 2(c) illustrates the cascade of biotinylated lipid, avidin, biotinylated anti-goat (targeting) IgG and goat (targeted) IgG adsorbed at the liquid crystal–water interface described below. At each step of fabricating the sensor and testing it against different antibodies, the liquid-crystal filled grid was rinsed with ultrapure deionized water, and then gently lowered onto a 0.5 ml droplet of the desired dispersion.

First, we prepared vesicles containing 2 wt.% Biotin-X-DHPE in DLPC and added water to create a vesicle suspension with a 1 mM lipid concentration. Unlike in other experiments where sensing the presence of the lipid is the primary aim [11,14,19], the goal here was merely to produce a dense lipid layer adsorbed to the surface. Fig. 3(a–c) shows the typical progression of film appearance upon addition of the lipid vesicles. Before the lipid reaches the LC interface, the texture is uniformly

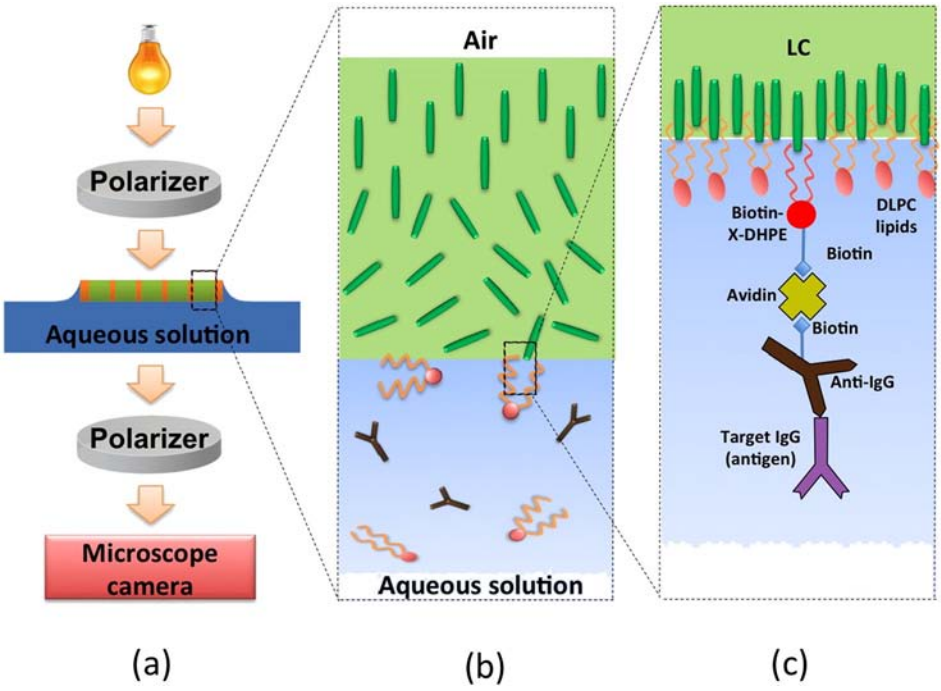

Fig. 2. Schematic illustration of the experimental method and the principle of operation. (a) Elements of the experimental setup; (b) close up of the liquid crystal with air (top) and aqueous (bottom) interface containing various chemical and biological analytes; (c) schematic of the decorated liquid crystal — aqueous interface studied in this work.

bright between circular polarizers. As the lipid vesicles open and attach to the liquid crystal interface, dark patches appear and grow; however, even after a long time (several hours), metastable birefringent domains persist, a characteristic feature of lipid-nematic liquid crystal interactions [13,25,26]. The formation of a stable uniform homeotropic texture can be facilitated by heating the liquid crystal to its isotropic phase and

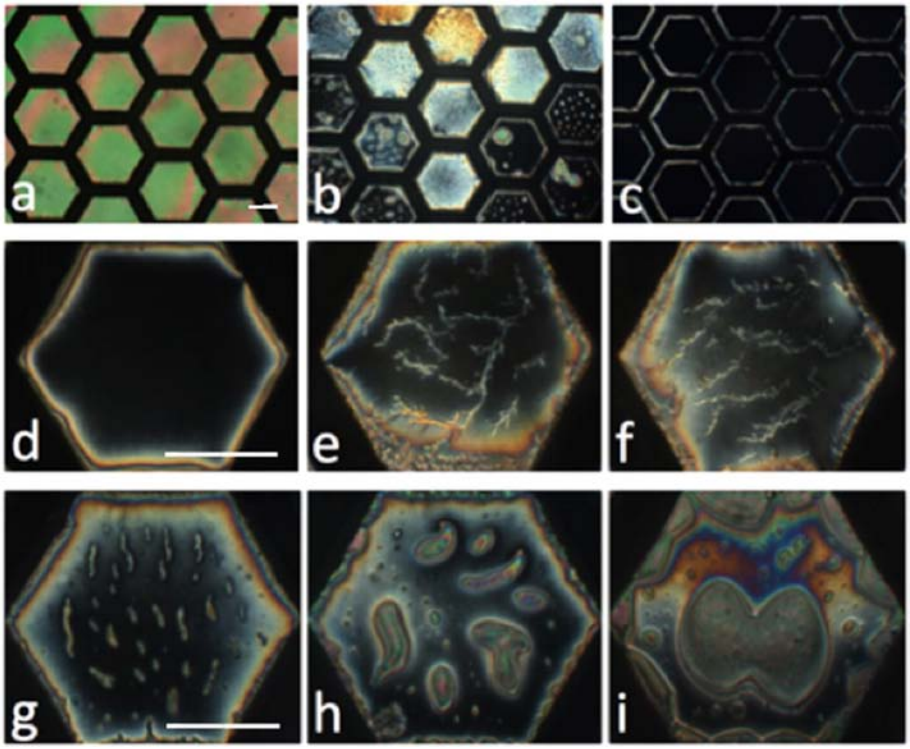

Fig. 3. Textures of a 5CB film contained within a 100-mesh TEM grid upon adsorption of DLPC and Biotin-X-DHPE. Scale bars indicate 100 μm. Top row: (a) a 5CB film immediately upon addition of the lipid showing hybrid alignment indicating that the lipid has not reached the interface, so the liquid crystal is in contact with water from one side; (b) the LC-lipid system after 30 min, showing the presence of metastable hybrid domains surrounded by homeotropic areas; (c) uniform stable homeotropic alignment after heating the nematic liquid crystal to the isotropic phase before cooling back to the nematic phase, thus causing the metastable planar domains to disappear. Middle row: Response of 5CB decorated with a monolayer of 98% DLPC and 2% Biotin-X-DHPE to neutravidin: (d) no neutravidin; (e) and (f) examples with 2 mg/ml concentration of neutravidin after 60 and 90 min, respectively. Bottom row: Response of 5CB decorated with a monolayer of 98% DLPC and 2% of Biotin-X-DHPE and neutravidin to biotinylated anti-goat IgG: (g) response of 10 mg/ml of biotinylated anti-goat IgG after 10 min; (h) example with 10 mg/ml of biotinylated anti-goat IgG after an additional 60 min; (i) example with 10 mg/ml of biotinylated anti-goat IgG after an additional 20 min.

cooling back to the nematic phase, as seen in Fig. 3(c). Such a homeotropic texture remained stable after rinsing the film with water and thus removing any unbound lipid.

Next, we placed the lipid-decorated film on a solution of neutravidin in Tris buffer at a 2 mg/ml concentration. The binding of the neutravidin to biotin resulted (Fig. 3(d–f)) in a characteristic dendritic texture [27, 28] resembling patterns created by two-dimensional diffusion limited aggregation [29]. Such a dendritic texture remained unchanged even 6 h after removing the sensor from the contact with the neutravidin solution. This binding step was followed by another rinse with deionized water before placing the lipid-decorated film on a drop of 5–10 mg/ml biotinylated anti-goat IgG in phosphate-buffered saline (PBS) and allowing the antibodies to attach to the avidin linkages. The response to the anti-goat antibodies is shown in Fig. 3(g–i). The birefringent domains formed by the anti-goat (targeting) IgGs have rounded edges and tend to fuse with each other. Both the tendency to fuse and the smooth boundaries suggest a relatively high line tension associated with the boundaries. As the domains fuse and grow, they tend to relax towards circular shapes to minimize their surface area. The growth process was halted, by rinsing with water, at a stage where round birefringent and dark homeotropic areas coexisted with area fractions ~50%. This dry biotinylated DLPC–neutravidin–anti-goat IgG decorated 5CB film represents the prefabricated sensor designed to be specifically sensitive to the goat IgG antigen.

The test results of this prefabricated sensor are shown in Fig. 4. Textures in the top two rows show the response to goat IgG at 10 mg/ml concentration in PBS (Fig. 4(a–d)). The goat antibodies (targeted IgG) change the appearance of the rounded domains produced by the anti-goat IgGs by making their boundaries jagged, indicating that the line tension of the domains decreased significantly. After an hour of contact with the goat IgG solution, almost the entire area of the LC sensor becomes bright, showing birefringent colors as seen in Fig. 4(d). Thus, both the shape and area fraction of the bright domains respond to the targeted IgG: these provide a readily visible and quantifiable detection mechanism.

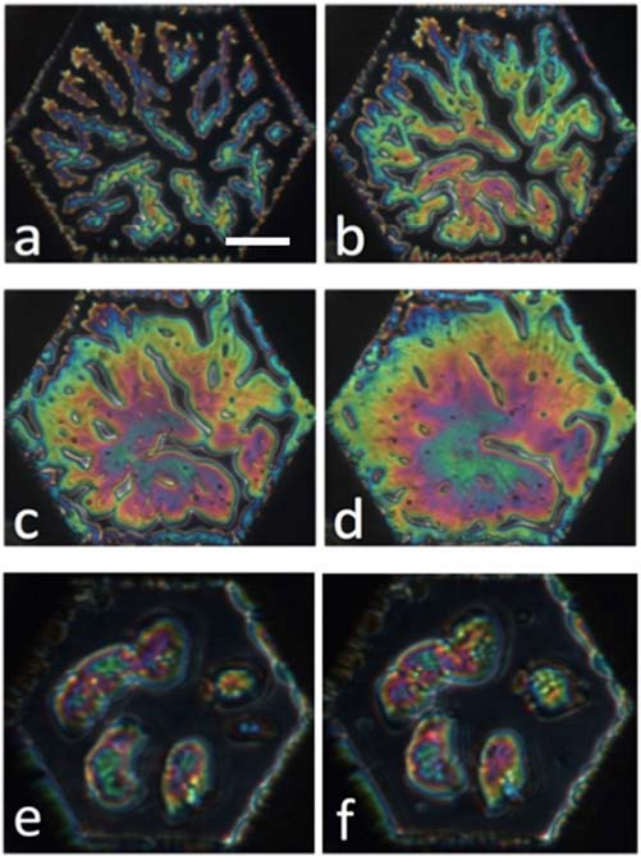

Fig. 4. Illustration of the LC sensor showing a specific response to goat IgG. Top and middle rows: Response of 5CB decorated with a monolayer of 98% DLPC and 2% Biotin-X-DHPE and biotinylated anti-goat IgG to goat IgG at 10 mg/ml: (a) after 20 min; (b) after 30 min; (c) after 40 min; (d) after 50 min. Bottom row: negative control experiment with rat IgGs (e) after 7 min; (f) after 31 min. Scale bar indicates 50 μm. Viewed between circular polarizers.

The crucial control experiment to test for specificity is to place a sensor built in the same way in the presence of biomolecules that do not specifically bind to the anti-goat IgG. The result of one such test, with rat IgGs in place of the goat IgGs, is given in Fig. 4(e, f): the area fractions of light and dark domains do not change, and the boundaries between the two remain relatively smooth. A similar lack of response was observed with rabbit IgGs. Furthermore, if the non-targeted IgG is rinsed from the cell, and replaced with the targeted IgG, a response like that in Fig. 4(a–d) is again observed. This combination of tests clearly indicates that the LC sensor responds specifically to goat IgGs only.

We performed a series of further control experiments:

1. The response was independent of the length of the rinsing steps. Rinsing steps of durations between 5 min and 6 h were employed, with no appreciable difference in response.
2. *No response* to either the avidin or to any of the IgGs was observed if the biotinylated lipid was *not* included in the initial lipid layer: the cell remained dark as shown in Fig. 3(c).
3. *No response* to any of the IgG's was observed if the step adding targeting IgG to the sensor cascade was omitted: the cell texture remained that of Fig. 3(f) in the presence of avidin and like that of Fig. 3(c) in its absence.
4. If the solution with the targeting IgG remained in contact with the cell for sufficiently long times, the texture became uniformly bright. Any further changes with addition of the targeted IgG were subtle. An approximately 50% coverage of bright domains induced by the targeting IgG showed a maximal response to the targeted IgG. Note that the bright domains formed by the targeting IgG addition step did become more compact with rinsing time, without measurably changing their area fraction; however, their response to the targeted IgG, in changing both shape and area fraction (Fig. 4(a–d)), did not depend on the rinsing time.
5. In addition to the extensively studied 10 mg/ml targeted IgG concentration, typical of serum concentrations [30], we also tested several lower (down to 5 mg/ml) concentrations. We found qualitatively similar responses, but with proportionally longer response times and larger errors.
6. Omitting the avidin addition step did *not* significantly affect (see figure) the sensor response to the targeted antigen. Both cases lead to a bright steady state, although the one without avidin is smoother (see Fig. 5).

Since both the biotinylated lipid and biotinylated targeting antibody were required for a response to any antibody (controls 2 and 3 above), it is difficult to understand what is happening in the absence of the separate avidin addition step. It is conceivable that some weaker, but sufficiently strong, bond than the biotin–avidin–biotin one is formed between the biotinylated targeting antibody and the biotinylated lipid layer; however, trace contamination by avidin, a common protein, seems more likely.

4. Summary

Specific detection of a serum antigen, goat IgG, through binding an antibody anti-goat IgG via biotin–avidin–biotin interactions was demonstrated. This interface did not respond to negative control antigens while showing a clear response to positive control antigens. It is expected that the same mechanism can be employed to make prefabricated sensors specifically sensitive to virtually any other antigen.

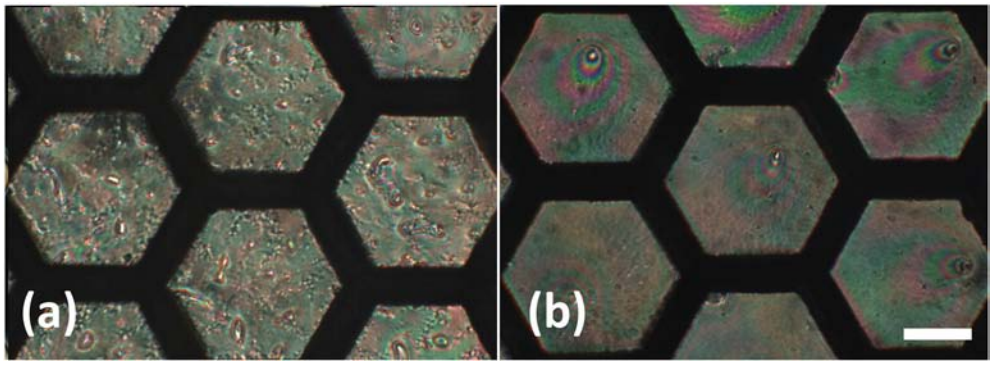

Fig. 5. Comparison of sensor response to biotinylated anti-goat IgG in the presence and in the absence of adsorbed neutravidin. (a) 31 min after introduction of biotinylated anti-goat IgG with neutravidin present; (b) 23 min after introduction of the anti-goat IgG, without neutravidin. Scale bar represents 100 μm. Images viewed between circular polarizers.

The potential of a sensor such as this is significant: the change of domain shape and coverage can be rapidly optically observed with only a few necessary components (the interface and biotinylated antibody) and the design of the sensor permits a response to be viewed in a small area. At the target concentration tested, both bright domain shape and coverage changed obviously within 5 min, and strikingly within 20 min. Although the limitations of the storage capabilities of this pre-fabricated rapidly-responding system have yet to be fully investigated, these results hold promise for sensors that can be used in food safety, or fighting epidemics.

Determining the quantitative evolution of bright domain shape and coverage with time over a wide range of targeted IgG concentrations will be the next step in developing this promising sensor. At sufficiently low concentrations we expect to reach a non-saturated steady state.

Acknowledgment

This work was financially supported by an NSF I-Corp site at Akron University and NSF DMR – 0907055. We are thankful to J. Budathoki, J. Redfearn, Dr. L. Showalter, Dr. G. Niehaus, and Dr. C. Woolverton for helpful discussions.

References

[1] R.M. Lequin, Enzyme immunoassay (EIA)/enzyme-linked immunosorbent assay (ELISA), Clin. Chem. 51 (2005) 2415–2418, http://dx.doi.org/10.1373/clinchem.2005.051532.
[2] P.R. Desai, L.H. Ujjainwala, S.C. Carlstedt, G.F. Springer, Anti-Thomsen-Friedenreich (T) antibody-based ELISA and its application to human breast carcinoma detection, J. Immunol. Methods 188 (1995) 175–185, http://dx.doi.org/10.1016/0022-1759(95)00246-4.
[3] M. Musiani, S. Venturoli, G. Gallinella, M. Zerbini, Qualitative PCR-ELISA protocol for the detection and typing of viral genomes, Nat. Protoc. 2 (2007) 2502–2510, http://dx.doi.org/10.1038/nprot.2007.311.
[4] F. Song, X. Sun, X. Wang, Y. Nai, Z. Liu, Early diagnosis of tuberculous meningitis by an indirect ELISA protocol based on the detection of the antigen ESAT-6 in cerebrospinal fluid, Ir. J. Med. Sci. 183 (2014) 85–88, http://dx.doi.org/10.1007/s11845-013-0980-4.
[5] Y. Ishizuka-Katsura, T. Wazawa, T. Ban, K. Morigaki, S. Aoyama, Biotin-containing phospholipid vesicle layer formed on self-assembled monolayer of a saccharide-terminated alkyl disulfide for surface plasmon resonance biosensing, J. Biosci. Bioeng. 105 (2008) 527–535.
[6] S. Sharma, J. Zapatero-Rodríguez, P. Estrela, R. O'Kennedy, Point-of-care diagnostics in low resource settings: present status and future role of microfluidics, Biosensors 5 (2015) 577–601, http://dx.doi.org/10.3390/bios5030577.
[7] S.V. Shiyanovskii, T. Schneider, I.I. Smalyukh, T. Ishikawa, G.D. Niehaus, K.J. Doane, et al., Real-time microbe detection based on director distortions around growing immune complexes in lyotropic chromonic liquid crystals, Phys. Rev. E Stat. Nonlinear Soft Matter Phys. 71 (2005), 020702(R), http://dx.doi.org/10.1103/PhysRevE.71.020702.
[8] S.V. Shiyanovskii, O.D. Lavrentovich, T. Schneider, T. Ishikawa, I.I. Smalyukh, C.J. Woolverton, et al., Lyotropic chromonic liquid crystals for biological sensing applications, Mol. Cryst. Liq. Cryst. 434 (2005), http://dx.doi.org/10.1080/15421400590957288 (259/[587]–270/[598]).
[9] G.D. Niehaus, Self-contained assay device for rapid detection of biohazardous agents, 7,060,225 B2, 2006.
[10] V.K. Gupta, J.J. Skaife, T.B. Dubrovsky, N.L. Abbott, Optical amplification of ligand-receptor binding using liquid crystals, Science 279 (1998) 2077–2080, http://dx.doi.org/10.1126/science.279.5359.2077.
[11] R.J. Carlton, J.T. Hunter, D.S. Miller, R. Abbasi, P.C. Mushenheim, L.N. Tan, et al., Chemical and biological sensing using liquid crystals, Liq. Cryst. Rev. 1 (2013) 29–51, http://dx.doi.org/10.1080/21680396.2013.769310.
[12] Y. Bai, N. Abbott, Recent advances in colloidal and interfacial phenomena involving liquid crystals, Langmuir 27 (2011) 5719–5738 (http://www.pubmedcentral.nih.gov/articlerender.fcgi?artid=3089817&tool=pmcentrez&rendertype=abstract).
[13] A.C. McUmber, P.S. Noonan, D.K. Schwartz, Surfactant–DNA interactions at the liquid crystal–aqueous interface, Soft Matter 8 (2012) 4335, http://dx.doi.org/10.1039/c2sm07483d.
[14] P. Popov, E.K. Mann, A. Jákli, Accurate optical detection of amphiphiles at liquid-crystal–water interfaces, Phys. Rev. Appl. 1 (2014) 034003, http://dx.doi.org/10.1103/PhysRevApplied.1.034003.
[15] L.N. Tan, R. Carlton, K. Cleaver, N.L. Abbott, Liquid crystal-based sensors for rapid analysis of fatty acid contamination in biodiesel, Mol. Cryst. Liq. Cryst. 1406 (2014) 37–41, http://dx.doi.org/10.1080/15421406.2014.917470.
[16] Y. Wang, Q. Hu, Y. Guo, L. Yu, A cationic surfactant-decorated liquid crystal sensing platform for simple and sensitive detection of acetylcholinesterase and its inhibitor, Biosens. Bioelectron. 72 (2015) 25–30, http://dx.doi.org/10.1016/j.bios.2015.05.001.
[17] D. Das, S. Sidiq, S.K. Pal, A simple quantitative method to study protein–lipopolysaccharide interactions by using liquid crystals, ChemPhysChem 16 (2015) 753–760, http://dx.doi.org/10.1002/cphc.201402739.
[18] L.N. Tan, N.L. Abbott, Dynamic anchoring transitions at aqueous-liquid crystal interfaces induced by specific and non-specific binding of vesicles to proteins, J. Colloid Interface Sci. 449 (2015) 452–461, http://dx.doi.org/10.1016/j.jcis.2015.01.078.
[19] W.G. Iglesias, N.L. Abbott, E.K. Mann, A. Jákli, Improving liquid crystal-based biosensing in aqueous phases, ACS Appl. Mater. Interfaces 4 (2012), http://dx.doi.org/10.1021/am301952f.
[20] S.R. Kim, N.L. Abbott, Rubbed films of functionalized bovine serum albumin as substrates for the imaging of protein-receptor interactions using liquid crystals, Adv. Mater. 13 (2001) 1445–1449, http://dx.doi.org/10.1002/1521-4095(200110)13:19<1445::AID-ADMA1445>3.0.CO;2-9.
[21] Y.P. Patil, S. Jadhav, Novel methods for liposome preparation, Chem. Phys. Lipids 177 (2014) 8–18, http://dx.doi.org/10.1016/j.chemphyslip.2013.10.011.
[22] S.S. Rathnayake, M. Mirheydari, A. Schulte, J.E. Gillahan, T. Gentit, A.N. Phillips, et al., Insertion of apoLp-III into a lipid monolayer is more favorable for saturated, more ordered, acyl-chains, Biochim. Biophys. Acta 1838 (2014) 482–492, http://dx.doi.org/10.1016/j.bbamem.2013.09.020.
[23] P. Popov, Liquid Crystal Interfaces: Experiments, Simulations and Biosensors, Kent State University, 2015 (http://rave.ohiolink.edu/etdc/view?acc_num=kent1434926908).
[24] J.-L. Guesdon, T. Ternynck, S. Avrameas, The Use of avidin–biotin interaction in immunoenzymatic techniques, J. Histochem. Cytochem. 27 (1979) 1131–1139.
[25] N. Lockwood, N. Abbott, Self-assembly of surfactants and phospholipids at interfaces between aqueous phases and thermotropic liquid crystals, Curr. Opin. Colloid Interface Sci. 10 (2005) 111–120 (http://linkinghub.elsevier.com/retrieve/pii/S1359029405000324 accessed September 27, 2011).
[26] M.I. Kinsinger, D.M. Lynn, N.L. Abbott, Nematic ordering drives the phase separation of mixed monolayers containing phospholipids modified with poly(ethylene glycol) at aqueous–liquid crystal interfaces, Soft Matter 6 (2010) 4095, http://dx.doi.org/10.1039/c0sm00080a.
[27] M. Khan, S.-Y. Park, Specific detection of avidin–biotin binding using liquid crystal droplets, Colloids Surf. B: Biointerfaces 127 (2015) 241–246, http://dx.doi.org/10.1016/j.colsurfb.2015.01.047.
[28] J.M. Brake, M.K. Daschner, Y.-Y. Luk, N.L. Abbott, Biomolecular interactions at phospholipid-decorated surfaces of liquid crystals, Science 302 (2003) 2094–2097, http://dx.doi.org/10.1126/science.1091749 (80-.).
[29] T.A. Witten, L.M. Sander, Diffusion-limited aggregation, a kinetic critical phenomenon, Phys. Rev. Lett. 47 (1981) 1400–1403, http://dx.doi.org/10.1103/PhysRevLett.47.1400.
[30] A. Gonzalez-Quintela, R. Alende, F. Gude, J. Campos, J. Rey, L.M. Meijide, et al., Serum levels of immunoglobulins (IgG, IgA, IgM) in a general adult population and their relationship with alcohol consumption, smoking and common metabolic abnormalities, Clin. Exp. Immunol. 151 (2008) 42–50, http://dx.doi.org/10.1111/j.1365-2249.2007.03545.x.